PROCEEDINGS OF SPIE

SPIEDigitalLibrary.org/conference-proceedings-of-spie

Ultra-low power stress-based phase actuation in TriPleX photonic circuits

Everhardt, Arnoud, Tran, T. Lan Anh, Mitsolidou, Charoula, Horner, Tom, Grootjans, Robert, et al.

Arnoud S. Everhardt, T. Lan Anh Tran, Charoula Mitsolidou, Tom R. Horner, Robert Grootjans, Ruud Oldenbeuving, Rick Heuvink, Douwe Geuzebroek, Arne Leinse, Chris Roeloffzen, René G. Heideman, "Ultra-low power stress-based phase actuation in TriPleX photonic circuits," Proc. SPIE 12004, Integrated Optics: Devices, Materials, and Technologies XXVI, 1200405 (5 March 2022); doi: 10.1117/12.2609405

SPIE.

Event: SPIE OPTO, 2022, San Francisco, California, United States

Ultra-low power stress-based phase actuation in TriPleX photonic circuits

Arnoud S. Everhardt[a1*], T. Lan Anh Tran[a1], Charoula Mitsolidou[a], Tom R. Horner[a], Robert Grootjans[a], Ruud Oldenbeuving[a], Rick Heuvink[a], Douwe Geuzebroek[a], Arne Leinse[a], Chris Roeloffzen[a] and René G. Heideman[a]

[a]LioniX International, P.O. Box 456, Enschede 7500 AL, The Netherlands

[1] These authors contributed equally.

*a.s.everhardt@lionix-int.com; phone +31 53 203 0053; lionix-international.com

ABSTRACT

We present ultra-low power stress optic actuators for high-speed switching in photonic integrated circuits using the standard silicon nitride TriPleX™ platform. The stress-optic actuator is created by a piezoelectric layer (lead zirconate titanate, PZT) on top of a Si_3N_4-based TriPleX™ waveguide in our standard Asymmetric Double Stripe (ADS) cross section. The top cladding thickness in between the actuator and the waveguide is chosen to achieve minimal optical loss (≤0.01dB/cm). The electrodes are placed on the top of- and directly below the PZT layer allowing the generation of a vertical electric field across the layer. This electrical field deforms the PZT layer by means of the piezoelectric effect. As a consequence of the PZT deformation stress is induced in the underlying waveguide. In this way, the refractive index of the waveguide is controlled by the stress-optic effect brought about by actuating the PZT layer. To demonstrate the stress-optic based phase actuation experimentally, a Mach-Zehnder Interferometer (MZI) is employed. The MZI is designed for operation at a wavelength of 1550 nm. We measure a half-wave voltage-length product (Vπ·cm) of 16 V·cm, while the half-wave-voltage length loss product ($V_\pi \cdot L \cdot \alpha$) is 1.6 V·dB only. The 2π phase shift would be at 42 V. The measured response time is 4.25 µs. The quasi-DC power dissipation is able to go down to 1 µW. Compared with conventional thermo-optic actuators these characteristics show a dramatic improvement, being a factor of 50 faster in terms of switching speed and a factor of 100 000 lower in terms of quasi-DC power dissipation. This makes stress-optic actuators an attractive choice for the next generation integrated photonic circuits where ultra-low quasi-DC power dissipation and/or fast switching time and operation in the MHz range are required.

Keywords: TriPleX, nitride, photonic circuit, PIC, phase actuation, PZT, low power, stress-optic

1. INTRODUCTION

Silicon nitride integrated photonic circuits (PICs) with very low propagation losses enable improvements in performance and reductions in size, weight and power consumption in diverse applications including LiDAR, tunable lasers, telecommunications and data centers[1]. As a passive waveguide material, silicon nitride offers uniquely low loss waveguides. It relies on the integration of actuators to enable the higher levels of functionality, such as switching reconfigurability and modulation, required in these applications. The optimal waveguide solution has been found in the LioniX International TriPleX™ Si_3N_4 waveguides with a SiO_2 cladding, in the standard Asymmetric Double Stripe (ADS) cross section (see also Figure 1a).

This need for efficient methods for the integration of actuators is particularly acute wherever large matrices of actuators are required, such as in the beam scanning chips of LiDAR systems or in microwave photonic Blass Matrix chips for high capacity broadband antennae[2].

Whilst several solutions for integrated actuators exist, their inherent drawbacks limit the usefulness of reconfigurable PICs. For example, the hybrid integration of active materials for signal modulation is inherently labor-intensive[3]. Another approach, direct electro-optic modulation, suffers from high optical losses in the actuator material, typically greater than 1 dB[4–6].

The most common integrated actuation method uses thermo-optic heating elements[7]. The heat generated by Joule heating in a metal strip causes an increase of the refractive index of the waveguides below. This method has two advantages over hybrid integration of modulators and electro-optic actuation. Firstly, the production is scalable, as the metal heaters are

Integrated Optics: Devices, Materials, and Technologies XXVI, edited by Sonia M. García-Blanco, Pavel Cheben, Proc. of SPIE Vol. 12004, 1200405 · © 2022 SPIE · 0277-786X · doi: 10.1117/12.2609405

deposited in wafer level processes. And secondly, the excess waveguide losses are kept below 0.01 dB/cm, because the actuators are outside of the light propagation area.

However, a major drawback of thermo-optic actuation is both its high average power consumption of >300 mW and minimum actuation speed of >100 µs. Power consumption of the actuator is a particular problem in LiDAR and microwave beamforming applications. In these chips, with their hundreds of actuators, power consumption per chip can nearly run to the order of kilowatts. This is prohibitive in the environments for which they are intended. For space based LiDAR or communications systems, power budgets are severely constrained. For ground based communications networks the cumulative power requirements of current beam forming chips is economically and environmentally unacceptable: the sheer number of antennas can number up to tens of thousands in a national network.

In this paper we describe the development of an efficient stress-optic refractive index actuator to drastically improve power consumption and switching speed for on-chip actuation. The method we present exploits the large piezoelectric effect of the material $PbZr_xTi_{1-x}O_3$ (PZT). This approach maintains the advantages of wafer level fabrication in terms of production scalability; it also maintains the minimal excess loss by being outside the light propagation area. Compared to thermo-optic actuation, it has drastically reduced power consumption to <1 µW and actuation speed to 4.25 µs.

The drawback of stress-optic actuation is the relatively low effect and larger interaction lengths required for a full 2π phase actuation in optical structures. This research builds on earlier work[8,9], and has improved the efficiency with a factor of two by using a smart production process to focus the stress more efficiently into the waveguide core. The half-wave voltage-length product ($V_\pi \cdot cm$) of 16 V·cm, so an interaction length of 1 cm is enough at an operating voltage of 16 V to provide the π phase actuation. In addition, a full 2π phase actuation would require 42 V due to a small nonlinearity. The use of a 1 cm electrode length highly feasible in commercial applications due to the low propagation loss in the TriPleX™ waveguides of <0.1 dB/cm.

In Section 2 we detail the design of the stress-optic PZT structure and the simulations that predict its improved performance as an actuator. In Section 3 we describe the experimental setup to enable the efficient phase actuator results. The conclusion and an outlook on how to further improve the stress-optic actuation is found in Section 4.

2. STRESS-OPTIC PHASE ACTUATOR DESIGN

The key element to the stress-optic effect is the piezoelectric material $PbZr_xTi_{1-x}O_3$ (PZT) and its large piezoelectric coefficients d_{33f} > 200 pm/V and e_{31f} > 18 C/m^2, which have been achieved using a wafer-scale Pulsed Laser Deposition (PLD) growth method built by Solmates[10–12]. These coefficients are much larger than in some other commonly used piezoelectrics like AlN (or Sc:AlN), for which the coefficient d_{33f} is only 5 pm/V.[13–15]. The typical drawback for using PZT is that it requires a poling operation, which is a process in which the ferroelectric polarization is aligned to the electric field. The poling voltage in these thin films of 1-2 µm thick PZT is only 5-10 V, while the voltages used for phase actuation are in the order of 40 V. Therefore, the PZT is automatically poled during operation and does not require special pre-treatment.

The actuation scheme used is the so-called top-bottom configuration (see Figure 1), in which an electric field is generated over the PZT layer. The electric field produces a displacement in PZT due to its piezoelectric effect (>200 pm vertical displacement per volt, hence d_{33f} > 200 pm/V). The surrounding material partially prevents this displacement, called ‘clamping’, and thereby a mechanical stress is generated in this structure. This stress propagates to the TriPleX™ waveguide materials Si_3N_4 and surrounding SiO_2 cladding, generating a change in the refractive index.

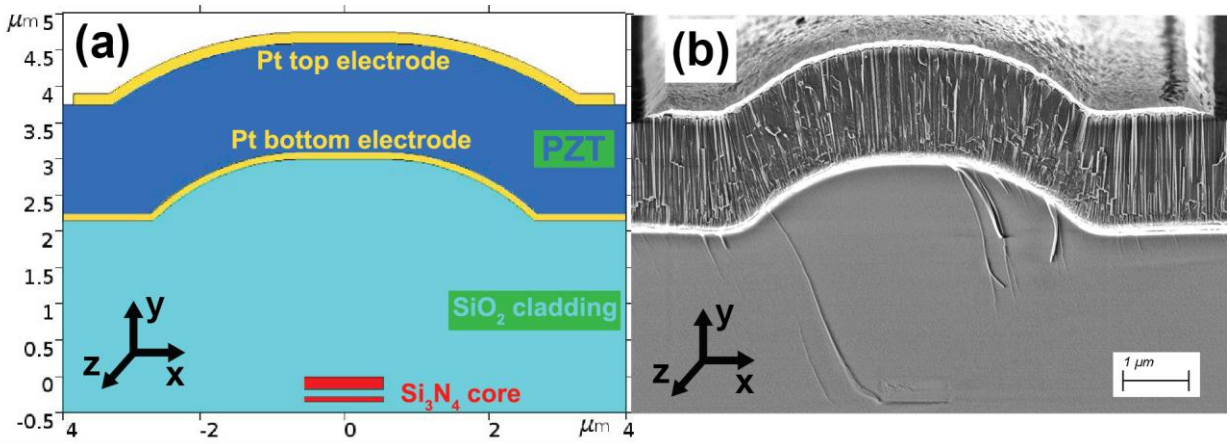

Figure 1. (a) Waveguide model for stress-optic PZT actuation of the waveguide. The bottom area contains the Asymmetric Double Stripe (ADS) TriPleX™ silicon nitride waveguide core (red), with SiO_2 cladding (light blue) surrounding it. The Si_3N_4 consists of two layers, the bottom layer 75 and the top layer 175 nm thick with SiO_2 in between. The waveguide width is 1.1 µm. The SiO_2 cladding is 3 µm thick between the top of the waveguide and the beginning of the PZT structure. The PZT material (dark blue), 1.5 µm thick, has a 100 nm Pt (yellow) bottom electrode which is the common ground for all devices on the wafer. Above the PZT, a top electrode (yellow) is applied locally to provide an electric field between the two electrodes (top-bottom) across the PZT. The dome-like structure is the natural shape of thick layers grown on dry-etched Si_3N_4 waveguides and the top electrode is chosen such that it fully covers this dome. (b) SEM photograph of the sketch shown in (a), displaying the microstructure of PZT.

The key element of the efficient stress-optic effect observed in these TriPleX™ waveguides is the natural formation of a dome structure. Etching the silicon nitride waveguides leaves a rectangular waveguide structure with a pedestal height of 1 µm, and subsequent deposition of 3 µm SiO_2 cladding material then produces this dome[1]. The reason why the dome is so effective is theorized in that it forms a sort of lens for the stress generated in the PZT and projects it efficiently on the waveguide core. A COMSOL model is constructed to understand the effect of the PZT piezoelectric effect on the phase shift that can be induced in the photonic circuit, shown in Figure 2. A voltage is applied between the top and bottom electrode, and the PZT deforms due to the piezoelectric effect: elongation along the y-direction and compression along the x-direction. This is hard-baked into such a top-bottom electrode configuration, since the voltages required for any sizeable phase shift are much larger than the poling voltage of the ferroelectric PZT material. So also negative voltages produce the same stress types.

The deformation of the PZT produces stress in the total structure, and this propagates to the waveguide core and surrounding cladding. The resulting refractive index changes can be calculated by[16]

$$\Delta n_x = C_1 \cdot \sigma_x - C_2 \cdot (\sigma_y + \sigma_z), \quad (1)$$

$$\Delta n_y = C_1 \cdot \sigma_y - C_2 \cdot (\sigma_x + \sigma_z), \quad (2)$$

$$\Delta n_z = C_1 \cdot \sigma_z - C_2 \cdot (\sigma_x + \sigma_y). \quad (3)$$

It calculates the refractive index changes Δn along the three directions for the σ values which are the stress components and the C_1 and C_2 the stress-optic coefficients of the materials. Stress builds up along all three directions, but only the refractive index change along the x-direction is important as this is sensed by the T_E mode of the light propagation, and in the simulation indeed 94% of the phase shift is caused by Δn_x. The stress-optic coefficient C_2 is much larger than C_1[8,16], so from Equation 1 it can be seen that Δn_x is mostly influenced by the y- and z-stress. The z-stress is low since the PZT is not able to deform (and produce stress) along this direction (since the phase actuator is more than millimeters long). So that only leaves the y-stress being able to significantly influence the phase actuator. Silicon nitride accounts for about 30% of the phase modulation and the cladding silicon oxide the remaining 70%.

In the y-stress figures from the COMSOL model, it can be clearly seen that the dome provides a lens function to focus the stress to the waveguide core and surrounding cladding (Figure 2a). The lens function is significantly reduced when the natural dome has been removed from the structure (Figure 2b). The stress is negative (compressive), so it provides a

densification, which increases the refractive index. In addition, a positive stress is also made right next to the stress-optic PZT element: this area does not receive an electric field and is elongated by the neighboring PZT, pulling the material below up to reduce the refractive index underneath. This opposite effect of about -10% can indeed be measured when misaligning the electrodes with respect to the waveguide and could be utilized in a smart optical scheme.

A voltage of 40 V on this structure in the COMSOL model predicts a 2.6π phase shift for an actuator length of 1 cm at a wavelength of 1550 nm for the dome structure, and 1.6π for the flat structure. The measurements are able to produce up to 1.9π for the dome and up to 0.8π for the flat structure. So the dome result matches the simulations quite well, while the flat structure is even less effective than predicted. This shows that the dome is absolutely required to achieve an efficient stress-optic phase actuator.

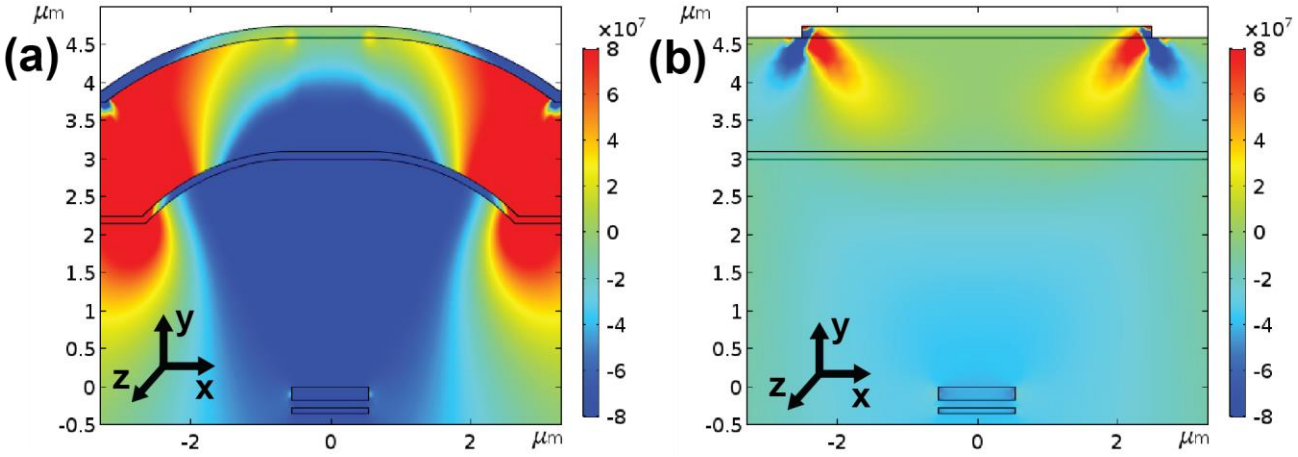

Figure 2. (a) The y-stress tensor induced in a typical TriPleX™ waveguide structure with a dome formed due to the fabrication process. The stress is given at the different positions because of a 40 V voltage applied, where blue shades are negative stress and red shades are positive stress, and the z-direction is the light propagation direction. (b) The y-stress tensor for a similar waveguide as (a), but the surface has been made flat to remove the dome. The electrode widths are optimized for each of the structures.

3. STRESS-OPTIC PHASE ACTUATOR RESULTS

The measurements are performed using a Mach-Zehnder Interferometer (MZI) configuration. It consists of a 50/50 directional coupler to split the light into two arms and a second directional coupler to mix the two signals to give either constructive or destructive interference. Laser light is inserted into one input port and measured on one output port, and the phase shift is π when the light goes from full constructive (max power) to full destructive interference (min power); and 2π when going back to full constructive interference. To achieve a higher accuracy measurement of the phase shift, a broadband light source and spectrometer are used with an asymmetric MZI (aMZI) to measure a spectral interference pattern with a Free Spectral Range (FSR) of 13.6 nm. The phase shift is characterized by the wavelength shift using a sinusoidal fit through the spectrum. Electrodes are deposited on top of the waveguides to probe either the top or bottom arm. The electrodes are 2 μm wider than the width of the dome structure in order to certain that the full effect of the dome is captured even on misalignment. In this way, misalignments up to 2 μm have been found to result in <5% change in the measured phase shift.

The progression of the phase shift as a function of voltage can be seen in Figure 3. A phase shift of up to 1.9π has been measured with an operating voltage of 40 V at an electrode length of 1 cm, which can be extrapolated to a 2π phase shift at 42 V. The half-wave voltage-length product $V_\pi \cdot$cm is 16 V·cm. This is less than half the voltage required for a 2π phase shift operation, because materials like PZT inherently reduce their piezoelectric coefficients above the poling voltage. This is captured in a small negative quadratic term to the polynomial fit in Figure 3. The piezoelectric coefficients are known to depend on the structural properties of the deposited PZT films[10–12], and indeed variations of the phase shift values between 1.1π to 1.9π have been measured, depending on the exact PZT microstructures.

A yield of 90% has been achieved which is expected to further increase with proper passivation of the electrodes. The yield was measured on >1000 actuators and had to show at least 80% of the required actuation. Repeated actuation cycles of >500 times influence the measured phase shift by less than 1%, showing low fatigue behavior. Repeated measurements weeks apart also provide phase shift values that differ by less than 1%, showing great long-term stability and a low dependence on environmental conditions[17].

The large advantages of stress-optic PZT over the traditional thermo-optic phase actuators were their ultra-low power consumption and speed. The power consumption is a function of voltage and leakage current. Being an insulator, PZT ideally has no current in DC operation, however it still shows small amounts of leakage current. The current density is 0.01-0.1 µA/mm^2 at a 40 V operation voltage. So the power consumption measures 0.1-1 µW for an electrode area of the bond pad, plus the typical actuation electrode of 1 cm length and 10 µm width.

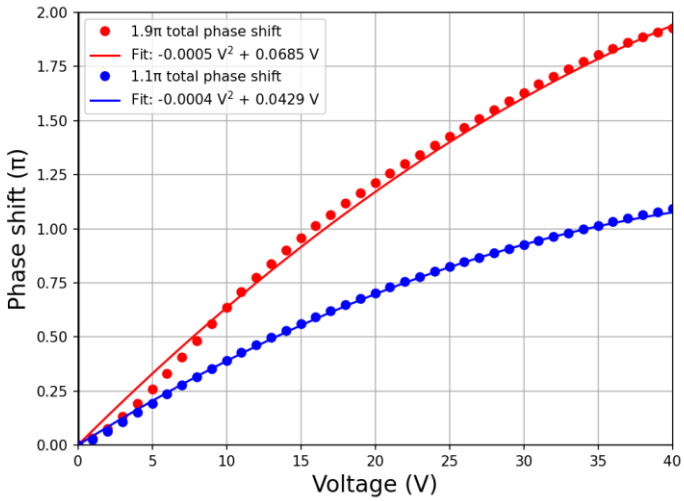

Figure 3. Phase shift as a function of voltage. The fit is a second order polynomial fit as the piezoelectric activity – and therefore phase shift - of PZT slowly decreases at values far above the poling voltage (10 V). The largest deviations to the fit are seen around the poling voltages as this is where PZT undergoes structural changes. Depending on the exact microstructure of PZT, phase shift values between 1.1π to 1.9π can be achieved.

Next, the step response of the PZT actuator was measured. The CW laser source was connected in one of the optical inputs of the MZI. The PZT phase shifter was driven from the electrical Arbitrary Waveform Generator (AWG) that generated a square waveform, which step response time shorter than the expected speed of the PZT phase shifter. In this way the measurement was not limited by the speed of the generator. The optical output of the MZI was connected to a high speed photodiode (PD) with 50 Ω matched load an 25 GHz bandwidth. The output of the detector was connected to an 4 GHz oscilloscope. The oscilloscope captured the step response (time-domain) of the MZI with stress-optic PZT actuator. The oscilloscope was set to a bandwidth of 100 MHz. Figure 4 presents the experimentally-obtained step response of the MZI-PZT actuator. The step response of the actuator corresponds to a 1st order linear system with time constant $\tau = 0.85$ µs. After five time constants of 4.25 µs the function reaches a value of 99% of its maximum value. This value corresponds to the switching speed of the actuator, which is a great deal better than the 100s of µs observed in thermo-optic phase actuators.

Finally, another great advantage is the small excess loss of <0.01 dB/cm induced by these PZT structures , because the phase actuator active component is far away from the waveguide. With the propagation loss of the waveguide, currently <0.1 dB/cm, the PZT excess loss contributes only an additional 10%. Therefore, the parameter to capture the PZT actuation in terms of light propagation efficiency is the half-wave-voltage length loss product ($V\pi \cdot L \cdot \alpha$), which is only 1.6 V·dB.

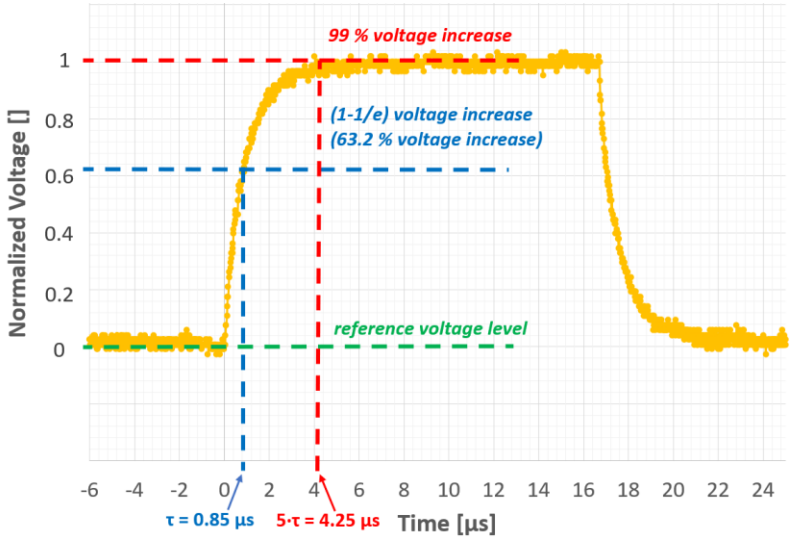

Figure 4. Step-response of a PZT stress-induced actuator: The step response of the actuator corresponds to a 1st order linear system with time constant τ = 0.85 µs. The measurement was performed by using a MZI with a PZT actuator in one of its arms (Figure 3), a high-speed photodiode to convert the optical signal at the MZI output to an electrical signal and an oscilloscope to capture the step response. The switching speed of the actuator was measured equal to 4.25 µs and it corresponds to the time that the function reaches 99% of its maximum value.

4. CONCLUSION AND OUTLOOK

Concluding, a PZT phase actuator has been developed and produced with a substantial reduction of a factor 50 in switching speed and a 100 000 times lower in quasi-DC power consumption, while keeping an ultra-low excess loss of <0.01 dB/cm. This makes these PZT stress-optic actuators an attractive choice for the next generation integrated photonic circuits where ultra-low quasi-DC power dissipation and fast microsecond switching time are required, for example LiDAR, tunable lasers, telecommunications and data centers.

Further improvements can be made in the PZT material quality and optical circuit design. Research in a higher efficient and more uniform PZT crystal structure needs to be performed in collaboration with the deposition machine manufacturer Solmates[18]. This will lead to higher performance, more uniformity, higher yield than the current 90% and lower power consumption than 0.1-1 µW. Secondly, a smart design will be able to use the negative stress and make use of the two arms of an MZI to configure a push-pull configuration: applying different stress on each of the arms to double the total phase shift. Lastly, different electric fiel

d configurations can result in better performance, for example changing the used top-bottom (vertical electric field) to a top-top (horizontal electric field) configuration. This should lead to opposite stress profiles, lower power consumption, higher possible actuation frequencies and most important of all, a more efficient actuator than the already impressive half-wave voltage-length product (Vπ·cm) of 16 V·cm.

ACKNOWLEDGEMENTS

This project has received funding from the European Union's Horizon 2020 research and innovation programme under grant agreement No 780502 (3PEAT) and No 870421 (SpaceBeam).

REFERENCES

[1] C. G. H. Roeloffzen et al., “Low-loss Si3N4 TriPleX optical waveguides: Technology and applications overview,” IEEE J. Sel. Top. Quantum Electron. 24, 4400321 (2018).

[2] C. Tsokos et al., “True Time Delay Optical Beamforming Network Based on Hybrid Inp-Silicon Nitride Integration,” J. Light. Technol. 39, 5845–5854 (2021).

[3] M. Theurer et al., “Flip-Chip Integration of InP to SiN Photonic Integrated Circuits,” J. Light. Technol. 38, 2630–2636 (2020).

[4] F. Eltes et al., “An integrated optical modulator operating at cryogenic temperatures,” Nat. Mater. 19, 1164–1168 (2020).

[5] K. Alexander et al., “Nanophotonic Pockels modulators on a silicon nitride platform,” Nat. Commun. 9, 4–9 (2018).

[6] A. Hermans, M. Van Daele, J. Dendooven, S. Clemmen, C. Detavernier, and R. Baets, “Integrated silicon nitride electro-optic modulators with atomic layer deposited overlays,” Opt. Lett. 44, 1112 (2019).

[7] Roeloffzen, C. G. H. et al. “Silicon nitride microwave photonic circuits.“ Opt. Express 21, 22937 (2013).

[8] Epping, J. P. et al. “Ultra-low-power stress-optics modulator for microwave photonics.“ Proc. SPIE 10106, 101060F (2017).

[9] Hosseini, N. et al. “Stress-optic modulator in TriPleX platform using a piezoelectric lead zirconate titanate (PZT) thin film.“ Opt. Express 23, 14018 (2015).

[10] Dekkers, M. et al. “The significance of the piezoelectric coefficient $d_{31,eff}$ determined from cantilever structures.“ J. Micromechanics Microengineering 23, (2013).

[11] Nguyen, M. D., Houwman, E. P., Dekkers, M. & Rijnders, G. “Strongly Enhanced Piezoelectric Response in Lead Zirconate Titanate Films with Vertically Aligned Columnar Grains.“ ACS Appl. Mater. Interfaces 9, 9849–9861 (2017).

[12] Nguyen, M. D., Tiggelaar, R., Aukes, T., Rijnders, G. & Roelof, G. “Wafer-scale growth of highly textured piezoelectric thin films by pulsed laser deposition for micro-scale sensors and actuators.“ J. Phys. Conf. Ser. 922, 012022 (2017).

[13] Zhu, S. et al. “Integrated ScAlN photonic circuits on silicon substrate.“ Opt. InfoBase Conf. Pap. Part F183-, 2020–2021 (2020).

[14] Xiong, C., Pernice, W. H. P. & Tang, H. X. “Low-loss, silicon integrated, aluminum nitride photonic circuits and their use for electro-optic signal processing.“ Nano Lett. 12, 3562–3568 (2012).

[15] Piazza, G., Felmetsger, V., Muralt, P., Olsson, R. H. & Ruby, R. “Piezoelectric aluminum nitride thin films for microelectromechanical systems.“ MRS Bull. 37, 1051–1061 (2012).

[16] Huang, M. “Stress effects on the performance of optical waveguides.“ Int. J. Solids Struct. 40, 1615–1632 (2003).

[17] Wang, J., Salm, C., Houwman, E., Nguyen, M. & Schmitz, J. “Humidity and polarity influence on MIM PZT capacitor degradation and breakdown.“, 2016 IEEE International Integrated Reliability Workshop (IIRW) vol. 3, 65–68 (2016).

[18] Solmates B.V., website: http://www.solmates-pld.com